

SCHOOL OF ENGINEERING AND MATERIALS SCIENCE

Queen Mary University of London

Modelling of Metastatic Cancer and its Treatment
using Swarm Intelligence Based-Control

DEN318 Third Year Project

by Joseph Zahar
Supervisor: Dr. Ketao Zhang

April 28, 2021

Declaration

School of Engineering and Materials Science

Third Year Project Den318

April 2021

I hereby declare that the project report entitled

"MODELLING OF METASTATIC CANCER AND ITS TREATMENT USING SWARM INTELLIGENCE BASED-CONTROL"

Was composed and submitted by me, Joseph Zahar, to Queen Mary University of London in partial fulfillment of the requirement for the award of my degree. I certify that this research report is my own work, where the work of the other has been indicated clearly and acknowledged in the text and in captions to table illustrations. This research is a record of bona fide project work carried out by me, under the guidance of Dr. Ketao Zhang, and has not been submitted for any other qualification or diploma.

Joseph Zahar

Signature of the Candidate

April 28, 2021

Joseph Zahar

Abstract

Considering the rise of frequency and severity of cancer-related deaths worldwide and the many side effects current treatments adduce, the emergence of novel therapies is of particular interest. This study investigates the use of swarm robotics and nanotechnology to target cancer cells autonomously and efficiently, focusing on exploring new control algorithms inspired by the combined behaviour of social animals. Localised self-organising networks that copy the behaviour of animals colonies is generally referred to as swarm intelligence. A first cancer growth model is developed through a cellular automaton based approach and validated using accurate cancer data and machine learning. The model is coupled to a second CA self-organising system of nanorobots that revealed some limitations. Four new control algorithms are generated and implemented in a specialised multi-agent system platform to test their efficacy. Numerical experiments carried out for different variables values demonstrated that the proposed systems are scalable and showed a precise targeted treatment since the search dominated algorithm consisting of 200 agents eradicated all cancer cells within 300s. Hence providing a potential therapy to treat cancerous cells, one of the most critical challenges of our time.

Contents

1	Introduction	7
1.1	Metastatic Cancer	7
1.1.1	Cancer Growth Models	7
1.1.2	Cancer Treatments	8
1.2	Nanotechnology	8
1.2.1	Nanoparticles in Cancer Therapy	9
1.3	Multi-Agent Systems	10
1.3.1	Swarm Robotics	10
1.3.2	Swarm Intelligence	11
1.4	Aims and Objectives	12
2	Cellular Automata Based Model of Cancer Growth	12
2.1	Cellular Automaton	12
2.2	Modelling of Cancer Growth	13
2.2.1	Assumptions	13
2.2.2	Initialisation	14
2.2.3	Rules-Governed Cancer Growth Model	15
2.2.4	Cancer Growth Experiments	15
2.3	Accuracy of the model	16
3	Modelling of Self-Organising Nanorobots	17
3.1	Design of Nanorobot for Drug-Delivery	17
3.1.1	Components & Function	17
3.2	Cellular Automata Based Model of Nanorobots	18
3.2.1	Assumptions & Initialisation	19
3.2.2	Rules: Nanorobots' Control Laws	19
3.2.3	Results & Future work	21
3.3	Multi-Agent based model of Nanorobots	22
3.3.1	Assumptions & Initialisation	22
3.3.2	Random Motion Algorithm	23
3.3.3	Flock Motion Algorithm	24
3.3.4	Search Dominated Motion Algorithm	24
3.3.5	Flock Dominated Motion Algorithm	25
4	Results & Discussion	26
4.1	Variables Investigation	26
4.1.1	50 Nanobots	26

4.1.2	100 Nanobots	27
4.1.3	150 Nanobots	28
4.1.4	200 Nanobots	29
5	Conclusions	31
6	Contributions & Acknowledgements	32
7	References	33
8	Appendix	38
8.1	Appendix A: Supplementary Work	38
8.2	Appendix B: Parameters of the simulations	38
8.2.1	Cellular Automata Parameters	38
8.2.2	Multi-Agent system Parameters	38
8.3	Appendix C: Algorithms Repository	39
8.3.1	Cancer Growth Algorithm	39
8.3.2	Accuracy of Cancer Growth Model	39
8.3.3	Cancer Population Plot	39
8.3.4	Nanorobot CA Algorithm coupled with cancer growth	39
8.3.5	Random Motion Algorithm	39
8.3.6	Flock Motion Algorithm	39
8.3.7	Search Dominated Motion Algorithm	39
8.3.8	Flock Dominated Motion Algorithm	39
8.3.9	Decontamination Floor Algorithm	39
8.3.10	Variable Analysis Algorithm	39
8.4	Appendix D: CA Simulations	40
8.5	Appendix E: Cancer growth Data	41

List of Figures

1	Nanoparticles for targeted drug delivery	8
2	Nanoparticles strategies to target cancerous cells	9
3	Swarm topology	11
4	Grid coordinate	14
5	Proposed cancer growth experiments	15
6	Representative plot of cancer Growth	16
7	Linear regression curve fitted into a patient's tumor data	16
8	Design of a Nanoparticle	18
9	Simplified version of the simulation	19
10	Single run of the treatment phase	21
11	Grid's organisation	22
12	Random motion algorithm simulation	23
13	Flock motion algorithm simulation	24
14	Search dominated algorithm simulation	25
15	Flock dominated algorithm simulation	25
16	Variable analysis for 50 nanorobots	26
17	Variable analysis for 100 nanorobots	27
18	Variable analysis for 150 nanorobots	28
19	Variable analysis for 200 nanorobots	30

List of Tables

1	Cellular states parameters	14
2	Parameters of the cellular automata cancer model	38
3	Parameters of the decontamination floor simulation.	38
4	Cancer growth data	41

List of Algorithms

1	Cancer growth rules	14
2	Nanorobots kinetics rules	20

Nomenclature

Abbreviations

CA	Cellular Automata
SR	Swarm Robotics
SI	Swarm Intelligence
ML	Machine Learning
MDEs	Matrix Degradative Enzymes
MMPs	Matrix Metalloproteinases

Cellular automata parameters

N	Normal cell	[1]
C	Cancerous cell	[0]
B	Grid's boundary cell	[100]
R	Nanorobots particle	[3]
r	Random generated number	[0,1]
t	Simulation time	1000 s
t_1	Cancer growth phase duration	100 s
t_2	Treatment phase duration	900 s
α	Probability that the cancer grows south	[0.5]
β	Probability that the cancer grows north	[0.3]
γ	Probability that the cancer grows east	[0.7]
δ	Probability that the cancer grows west	[0.6]
$cell^t$	Cell state at time t	
$cell^{t+1}$	Cell state at time t+1	

Multi-agent system parameters

r_v	Robots radius of vision	[0,100]
ν_r	Linear velocity of robot	[0,1]
D_{min}	minimum distance between robots	[3]
η	Swarm alignment variable	[0,100]
T	Total number of robots	[0,200]

1 Introduction

1.1 Metastatic Cancer

Metastatic cancer is defined as cancer growth in a primary site before spreading to other parts of the body via the blood or lymph system (Schroeder et al., 2011). Cancer arises from the mutation of crucial genes in a set of healthy cells and develops into a solid tumour due to abnormally rapid proliferation (Ramis-Conde, Chaplain and Anderson, 2008). This study will first investigate the invasion-metastatic process and build a spatiotemporal simulation to provide a concrete visual tool to understand this biological process. We will also inspect a new potential treatment of the malignant cells through nanobots targeted drug delivery and design three different algorithms to control the kinetics of the agents. The driving force in this study is that metastatic cancer represents a significant challenge nowadays, being the most cancer-related death worldwide. This disease has a significant impact on society and figures among the leading causes of death, accounting for 9.6 million deaths in 2018 (Ferlay et al., 2013). Moreover, cancer's economic influence is drastically growing as the entire annual pecuniary expense of cancer in 2010 was valued at nearly US 1.16 trillion (Stewart BW, 2014).

1.1.1 Cancer Growth Models

Many scientists throughout the years have investigated the modelling of cancer spread. Mathematical frameworks were designed to artificially replicate cancer cells proliferation using sets of ordinary and partially differentiated equations (Franssen et al., 2019). However, these models have to consider many factors, including the presence of matrix-degrading enzymes (MDEs), the probability of apoptosis (programmed cell death), the diffusive and haptotaxis movement of cancer cells, invasive travel, and the risk of death inside the vascular network. Over time, many factors have been implemented to examine these various effects in more detail; a primary one-dimensional spatially specific model was introduced, succeeding new ordinary differential equation (ODE) models, describing spatiotemporal acid-mediated invasion through a framework of reaction-diffusion-taxis (Natasha K et al., 1996). Another famous study had focused on designing a continuum PDE model focusing on haptotaxis (Anderson et al., 2000), which was the first to expand modelling to a two-dimensional environment. Further non-local mathematical models have been proposed, including cellular automata paradigms (Kansal et al., 2000), restricted interactions in the PDE model (Armstrong et al., 2006), a probabilistic Markov Chain/Monte Carlo framework to analyze multidirectional tumour growth (Newton et al., 2013) and a patient-statistics-based engaging Markov Chain model (Margarit D. H. & Romanelli L. 2016). Finally, one of the most recent mathematical models for modelling

the abnormal proliferation of tumoral cells was developed and published by Linnea C. Franssen et al. in 2019, introducing a new spatially explicit model combining all the invasion-metastasis processes and factors (Franssen et al., 2019).

1.1.2 Cancer Treatments

The increasing scope of widely available cancer treatments evolves rapidly (Zhang et al., 2007). The most common type of therapies alongside surgery treatment are chemotherapy and radiotherapy (Arruebo et al., 2011); however, they present many side effects that may impact drastically the patient's well being, physical health, and emotional state (Pearce et al., 2017). Consequently, other types of treatments are emerging with promising results, such as immunotherapy, targeted therapy, hormone therapy, stem cell transplant, nanostructure-based therapeutics, and many more (Pucci, Martinelli, and Ciofani, 2019). The evolution and development of new solutions against cancer provide hope of complete remission while enhancing the patient's quality of life. Modern approaches like radiation therapy and chemotherapy often end up attacking more healthy cells than malignant ones (Arruebo et al., 2011).

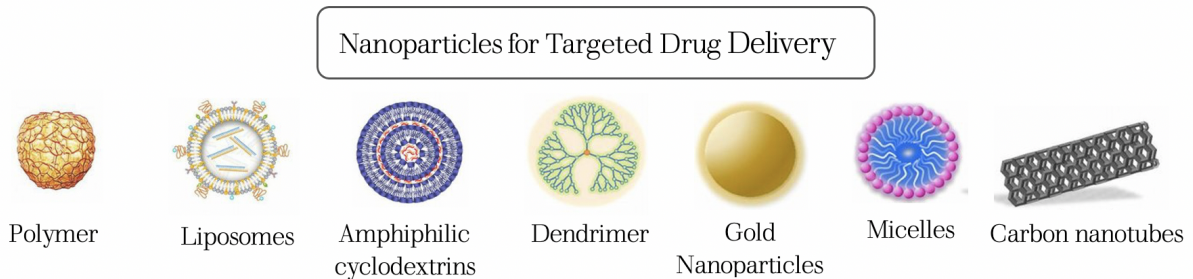


Figure 1: Different types of nanoparticles for targeted drug delivery (Mc Carthy et al., 2015)

The treatment method introduced in this paper is based on nanotechnology for cancer drug delivery via nanoparticles embedded in nanorobots. In fact, in the last decade, a large number of new nanostructure designs were developed to ensure targeting, prevention, and diagnosis of cancer, see figure 1 mentioned in Mc Carthy et al., 2015. This study will inspire from these mathematical frameworks for our spatiotemporal multi-grid model to produce a simplified and concrete simulation of cancer growth while introducing a new treatment method using nanotechnology.

1.2 Nanotechnology

Nanotechnology is a study field that includes structures, tools, and systems with innovative features that can act on the atom and molecule level (Bayda et al., 2019). Most

vital biological processes, including those that lead to cancer, occur at the nanoscale (National Cancer Institute, 2017). In current years, microengineering has been employed in human well-being with potential results, especially in tumour treatment (Bayda et al., 2020). Nanotechnology provides researchers with the opportunity to control macromolecules during the early stages of cancer progression, where molecular changes occur only in the cells genetic program (nucleus).

1.2.1 Nanoparticles in Cancer Therapy

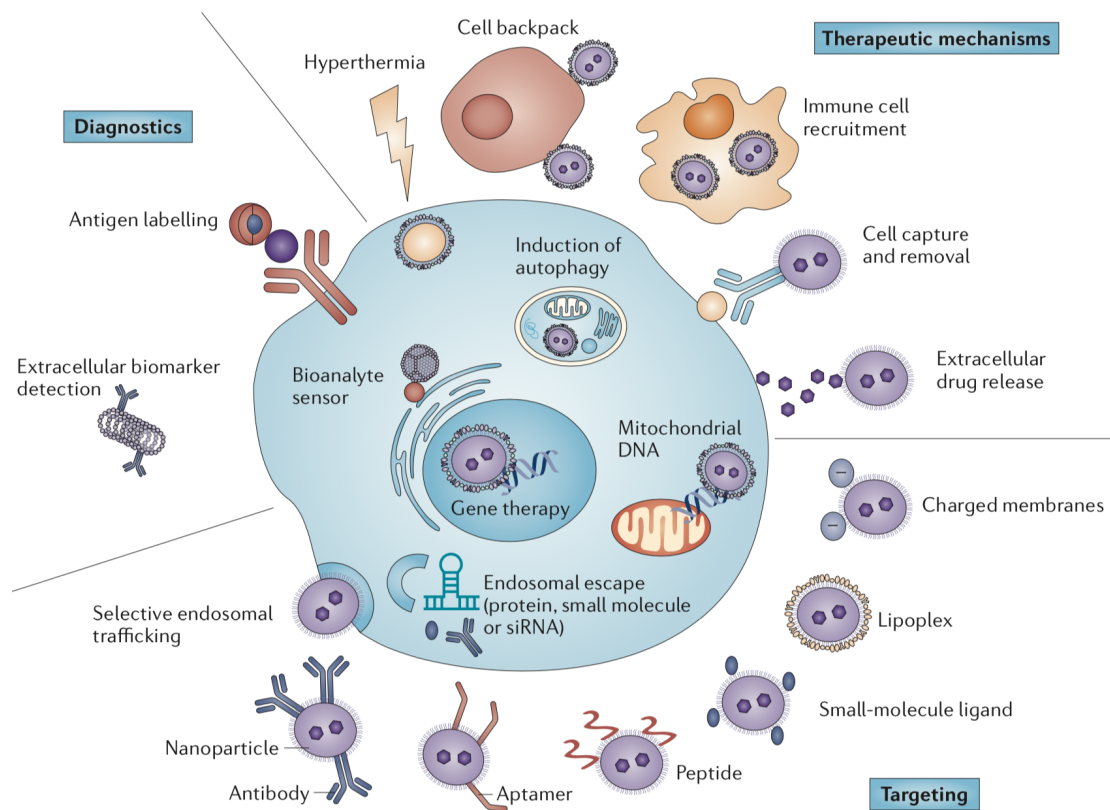


Figure 2: Nanoparticles strategies to target cancerous cells. This figure outlines the different techniques available for targeting, diagnostic and therapeutic mechanisms when in contact with tumoral cells. (Schroeder et al., 2011).

Nanoparticles have been the domain of concern for the last decade. They can provide rapid and sensitive detection of cancer-related molecules while generating highly effective treatment (National Cancer Institute, 2017). The detection process involves binding of the nanoparticles to the cancer cells surface antigen via trans-membrane molecules. This procedure is related to the tissue engineering and regenerative medicine field of research. Professor David Williams refers to tissue engineering as the process of "Persuading the body to heal itself by the delivery of molecular signals, new cells and supporting structures"

(Van Dijkhuizen-Radersma et al., 2008). These therapies can vary from inducing molecular signals to targeted cells, causing their apoptosis (degrading them), interfering with the genetic program, and delivering chemical drugs (Brannon-Peppas and Blanchette, 2012). Some novel and current strategies are presented in figure 2. The process of drug delivery via nanoparticles have been tested *in vivo* for many types of applications, and many substances are under investigation for cancer therapy (De Jong and Borm, 2008). Moreover, the development of nanorobots carrying these nanoparticles could lead to ground-breaking and life-saving discoveries for the treatment of patients achieved without any interaction with the healthy normal cells, hence overcoming conventional chemotherapies limitations (A, D and J, 2018). The nanorobots will potentially differentiate between cancerous and normal cells by monitoring their membrane antigens performed using chemotactic sensors attuned to the specific antigens on the target cells.

We will explore the fascinating field of nanotechnology to develop a possible treatment to stop the spread of metastatic cancer and compute this solution in our final simulation, assisted by a swarm intelligence control algorithm.

1.3 Multi-Agent Systems

Multi-Agent systems is a fast-developing and promising field, also defined as an interconnected system of operators that cooperate to obtain solutions to quandaries past the individual capacity of each agent (Ahmad, 2002). Agent-based technologies are generally used to solve complex problems, especially in swarm robotics, by interacting with the external environment and cooperating with the rest of the members (Wood and DeLoach, 2001). Combining the partial capability of each agent to perform its function enables to build intelligent and solid applications, providing enhanced flexibility to the system (Tinoco, Lima and Oliveira, 2017). This section is the pinnacle to aid the algorithmic developments in controlling our swarms of nanobots responsible for designing an efficient cancer treatment by creating a loose network within the group.

1.3.1 Swarm Robotics

Consequently, swarm robotics (SR) is a paradigm of multi-agent systems implemented into robotic systems using the right tools to generate synergy among the swarm agents, hence creating a dynamic global system capable of automated recognition of patterns by experience (O'Rourke and Toussaint, 2017). Swarm robotics define the self-organisation of a multi-robotic system that coordinates within the swarm based on a set of simple rules to achieve a more complex overall task in a decentralised way (Navarro and Matía, 2013). Unlike standard distributed robotic systems, SR systems have the advantage and

ability to enhance the system's overall performance by varying the number of robot agents without the need to reprogramming the agents (Innocente and Grasso, 2019). The swarm of robots can only find a solution to the addressed problem by working in collaboration, as they have limited individual capabilities relative to the task, hence inducing a collective behaviour within the swarm (Reséndiz-Benhumea et al., 2019). On the other hand, swarm robotics can be inspired by social insects' collective behaviour such as ants, birds flock, bees colony, termite mound or wasps nest, where each entity of the colony is not guided or informed of the overall situation. This kind of behaviour is also known as stigmergy, referring to direct local coordination or indirectly through the environment acting as a state memory (Innocente and Grasso, 2019). Stigmergy is usually considered a platform to swarm intelligence to design the rules for the interactions between agents to obtain the desired system's behaviour (Duan, Zhu and Huang, 2012). Therefore, we will investigate the behaviour of social insects to build a desirable control system and rules for our swarm of nanorobots to treat cancer efficiently via swarm intelligence (SI).

1.3.2 Swarm Intelligence

Swarm intelligence (SI) is a subsidiary of the artificial intelligence discipline that derives from the intelligence emerging from redistributed and self-organising systems with no main direction, a method by which logical exemplars appear from localised exchange among smaller parts of the network (Reséndiz-Benhumea et al., 2019). This collective intelligence is perceived in colonies of social animals that cooperate narrowly with each other and their surroundings, causing the appearance of general patterns (Duan, Zhu and Huang, 2012). Emergence, complexity, self-organisation and stigmergy present the roots and the primary explanatory concepts underlying SI. Furthermore, a combination of interactions, stochasticity, and feedback loops is essential for the system to become unchanged and robust to any disturbance while allowing proper communication among agents and enlarging the pool of knowledge within the swarm Figure 3 (Innocente and Grasso, 2019).

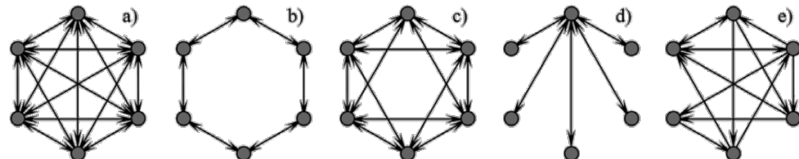


Figure 3: Different neighbourhood structures and topology generally used to determine the level of connection within the swarm. a) represent an overall topological order where every member is associated to the other, b) pair neighbours hoop topology, c) four neighbours hoop topology, d) wheel topology, and e) random topology (Innocente and Grasso, 2019).

Finally, this research is driven by the need to provide a straightforward visualization tool to clarify the complex process of cancer and raise awareness over the burden that it represents nowadays. There are plenty of innovative ways to use nanotechnology to treat and heal cancer, to the extent of delivering treatment in ways never imagined before. This new type of medical care is still under development and is very promising for the future of medical treatment and prognostic. This study is compelled by the opportunity to combine medical treatment and swarm robotics to innovate cutting edge solutions in an emerging world. In the next section, we will discuss this project's specific aims and, more specifically, the main goal we hope to achieve.

1.4 Aims and Objectives

Our project aims to design, develop, and build a solid computational model in terms of a multi-agent system that must reproduce the evolution of a tumour in a host tissue before metastasizing in other sites of the body. We will also explore a new approach to treatment using nanotechnology and model the outcome in our simulation. Another aim of this project is to generate different control algorithms based on swarm robotics to guide the nanoscale construct path to the most effective route to heal the tumour. Here, valuable and popular bio-inspired swarm intelligence models have been presented to solve complex solutions. The most effective model and assumptions will be explored to create an adequate framework for our visual simulation. Our main goal is to merge these three research fields to achieve a new interactive visualization tool that models most effectively metastasis cancer and its treatment via a controlled swarm of nanorobots.

2 Cellular Automata Based Model of Cancer Growth

2.1 Cellular Automaton

First acquainted by Von Neumann in 1951, cellular automata (CA) is considered one of the adequate tools to stimulate and analyse complex environment and test future solutions to the latest problems (Cerruti, Dutto and Murru, 2020). Cellular automata (CA) involves modelling a specific event based on a defined set of rules in a two-dimensional cellular grid to describe the development of a population. Building a solid CA simulation requires a representative of physical phenomena in the real world, such as space, state, and time discretised. Each cell of the grid possesses a computational apparatus that will change or stay unaffected depending on the cell's neighbourhood at each iteration and the previously defined rules (Muzy et al., 2005). Most cancer growth models present in the literature have been restricted to two-dimensional grids, being more feasible and straightforward in

computation and since tumour cells generally grow in an oblate spheroid shape (Butler, Mackay, Denniston and Daley, 2014; Dütting and Dehl, 1980). This section will examine a cellular automaton based algorithm to model accurately tumour growth.

2.2 Modelling of Cancer Growth

The following cancer growth simulation and algorithm were implemented and generated using Python programming language. The algorithm was inspired and adapted from (Hadeler and Müller, 2017), (Medium, 2019) and (Shiflet, 2006) based on cellular automata and their applications. In this section, we use a pseudo-code to describe our procedure and methods of implementation.

2.2.1 Assumptions

Some critical assumptions need to be put into place before running the model. As stated and displayed in previous mathematical and computational models (Gerisch and Chaplain, 2008; Ramis-Conde, Chaplain and Anderson, 2008; Anderson et al., 2000; Murphy, Jaafari and Dobrovolny, 2016), cancer evolution is a multi-scale phenomenon that involves a complex cascade of inter-related processes. These processes include the presence of matrix degradative enzymes (MDEs) and a large family of matrix metalloproteinases (MMPs) that are both implicated in the tumour invasion and growth by degrading the surrounding extracellular matrix (ECM) (Gerisch and Chaplain, 2008). Also, the CA simulation evaluates a pre-defined grid size that is not suitable for our simulation since a tumour expands due to unchecked cell growth, i.e. uncontrolled proliferation of the cells. As the number of cells is constant in the grid, the cancer cells will appear to contaminate the normal cells instead of pushing out and compressing them. This study aims to provide a simple visualisation tool to model cancer growth while investigating swarm robotics-based treatment, thus the need to introduce a set of assumptions suitable for a CA environment:

1. MDEs and MMPs are not considered in the simulation.
2. The effect of vascularisation and nutrients delivery on cancer cells are not studied.
3. We assume the normal cells being pushed out and that the cancer cells are dividing out of control.
4. The grid's borders bound cancer growth to the specific dimensions of the grid.

2.2.2 Initialisation

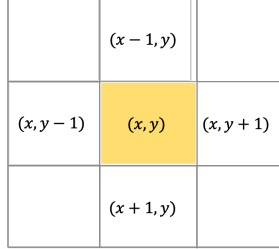


Figure 4: Grid coordinate

Cellular State	Number	RGB Color
Normal	0	[255, 209, 178]
Cancerous	1	[10, 10, 10]
Boundary	100	[248, 248, 255]
Blood	50	[255, 0, 0]
Robots	3	[255, 255, 0]

Table 1: Cellular states parameters

Algorithm 1 Cancer growth rules

```

1: for  $t_i \in \{1, \dots, t_1\} \forall t > 0$  do
2:   for all  $cell \in Grid$  do
3:     if  $cell^t(x, y) = C$  then
4:        $cell^{t+1}(x, y) = C$ 
5:       if  $cell^t(x + 1, y) = N \cap P(r \cap [0, 1]) > \alpha$  then
6:          $cell^{t+1}(x + 1, y) = C$ 
7:       end if
8:       if  $cell^t(x - 1, y) = N \cap P(r \cap [0, 1]) > \beta$  then
9:          $cell^{t+1}(x - 1, y) = C$ 
10:      end if
11:      if  $cell^t(x, y + 1) = N \cap P(r \cap [0, 1]) > \gamma$  then
12:         $cell^{t+1}(x, y + 1) = C$ 
13:      end if
14:    end if
15:  end for
end for

```

A two-dimensional grid of square cells is generated with $n \times n$ rows and columns depending on the desired pixel density, parameters and space of the simulation. The grid size and the number of initial cancer cell randomly located in the initial grid at t_0 are first entered independently before assigning blood cells, defining the tissue's environment. The cellular grid is composed of a large matrix of numbers, where each number defines a specific cell type and colour, see Table 1. The main temporal parameters are defined to delimit the two phases of our computational simulation: The cancer spread phase and the treatment phase described in section 4. Initially, all the matrix numbers are set to 0, defining the normal healthy tissue cells before randomly assigning one to three cancer cells to the

matrix. Finally, four variables representing the spread probabilities of the tumour at each direction (North, South, East, West) of the central cell at each iteration are defined (table 2), thus initiating a unique cancer growth at each simulation.

2.2.3 Rules-Governed Cancer Growth Model

Like any cellular automaton, rules are established to characterise each scenario with a specific outcome depending on the type of neighbour cells. A similar example of a rule-governed cellular automaton is Conway's Game of Life by John Conway in 1970 (Gardner, 1970), where three genetic laws govern the simulation (Gardner, 1966): birth, death and survival. Each cell interacts with its four adjacent neighbours as shown in Figure 4. In this model, five laws rule the outcome of cancer growth and are presented in Algorithm 1.

2.2.4 Cancer Growth Experiments

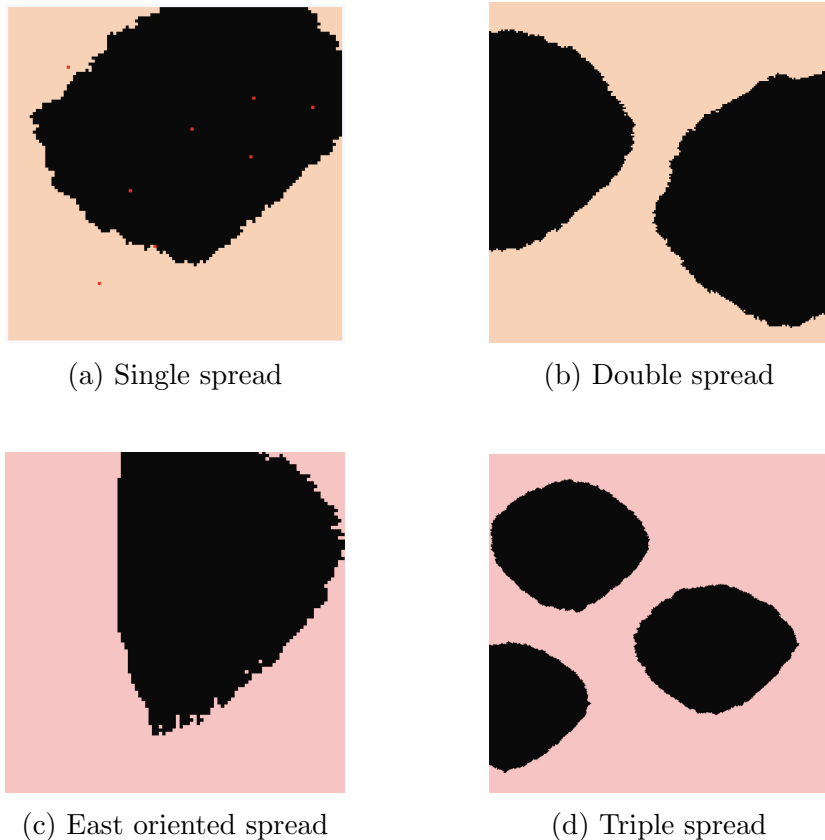


Figure 5: Proposed cancer growth experiments: (a) Represents the growth of cancer from one initial cell and a vascularised network in a 110×110 grid, (b) Demonstrates the spread of two initial cancerous cells in a 200×200 grid, (c) Represents the spread of a tumour specifically to the right direction in a different coloured grid in a 100×100 grid, (d) Triple spread of cancer in a 500×500 grid.

Using the manipulation of probabilistic-based rules as shown in Algorithm 1, we could reproduce a dynamic and realistic 2D environment for tumour growth. In fact, the algorithm and function implemented allowed a wide range of options, starting from single to multiple cancer sites, different tumour sizes, different spread direction, different colours and distinct pixel density. These distinct type of experiments are presented in Figure 5 and build up a base for the next phase of our experiment, allowing us to test the efficacy of a potential treatment and its effect. In the following subsection, the accuracy of the cancer growth model is measured before applying the control algorithm of the nanorobots.

2.3 Accuracy of the model

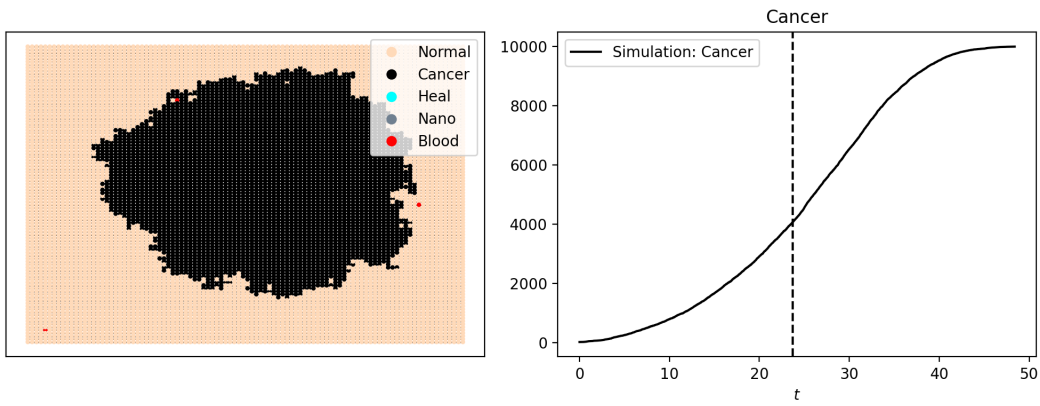


Figure 6: Representative plot of cancer Growth

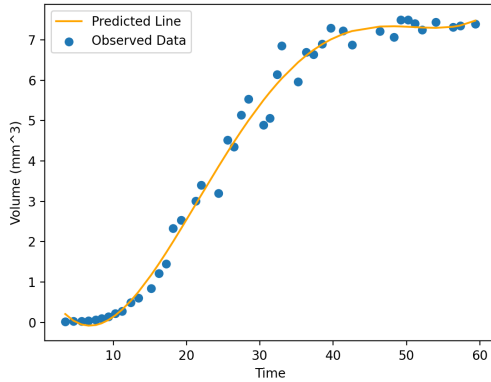


Figure 7: Linear regression curve fitted into a patient's tumor data

In order to proceed to the next phase of this study, it is primordial to ensure that the computational model is valid and similar to real-life tumour growth in any typical cancer patient. Concrete models of tumour growth would allow researchers to estimate the

potency of treatments and optimise therapy methods. The dataset provided in table 4 is secured from a Chinese hamster V79 fibroblast tumour cell line consisting of forty-five volume measurements through a period of 60 days (Wang J., 2018). The tumour volume was plotted against time, and a linear regression curve (Machine Learning) elevated to the fourth polynomial degree was fitted through the scatter plot as shown in Figure 7. To check the accuracy of our model, a new algorithm was designed using EoN (Epidemics on Networks), a Python library for analytic estimation adapted from (Miller and Ting, 2019), to obtain a representative plot of our simulation Figure 6. By comparing both figures, we can see that the trend is similar and almost identical, hence validating our model and confirming its similarity to real-life cancer growth. Here is the equation of the curve fitting the provided data:

$$f(t) = 1.4 - 0.467t + 4.25 \times 10^{-2}t^2 - 9.508 \times 10^{-4}t^3 + 6.65 \times 10^{-6}t^4 \quad (1)$$

3 Modelling of Self-Organising Nanorobots

3.1 Design of Nanorobot for Drug-Delivery

By using the linear regression model to understand tumour growth, a cancer treatment solution at the nanoscale can be explored via the modelling of nanorobots. Inspired by the self-organisation of social animals and swarm intelligence algorithms, this study will inspect the outcome of innovative control algorithms on cancer cells' chemical apoptosis. The first part will elaborate on the design and components of the nanobots in question to ensure reliable delivery of the nanoparticles/drugs. Then, we will further develop the previous cellular automata algorithm by implementing a control system based on a set of rules. Finally, four new algorithms are generated in a specialised multi-agent system platform [Netlogo].

3.1.1 Components & Function

A detailed study of the parts and components of a nanorobot is beyond the scope of this paper. However, many studies have investigated the functions and manufacturing technologies to produce the desired nanostructures (Chythanya C. Kutty et al., 2020; Senanayake et al., 2016; A, D and J, 2018; Madou, 2012). Further development in electronic and microprocessor manufacturing provides essential resource suitability in nano-computational systems while allowing particle systems to implement into nano-computers (Dolev, Narayanan and Rosenblit, 2019). Five main components are prescribed to achieve adequate control of the robots and reliable sensory detection, including nano-motors, bio-

detectors, sensors, encapsulated nanoparticle drugs and microprocessors (Chythanya C. Kutty et al., 2020). The functions sustained by these parts are similar to the functions attained by the ribosome, a piece of molecular machinery present in the cytoplasm of any living cell (A, D and J, 2018). The key mechanism behind this treatment is build on the nanoparticles encapsulation inside nanorobots, which their role in cancer therapy and treatment have been explored beforehand in section 1.2.1. Each nanorobot is responsible for detecting cancer cells through bio-detectors/molecular sensors and subsequently delivering adequate nanoparticles. These nanorobots also can sense each other via sensors, granting the formation of an interconnected artificial network that can be used in our favour by designing novel control algorithm and efficient treatment. A 3D example of the nanoparticle confined is presented in figure 8 and designed using Blender software.

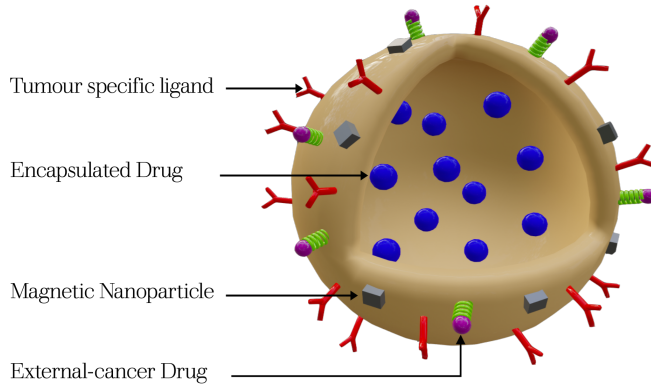


Figure 8: Schematic representation of a nanoparticle. The design was adapted from (Praetorius and Mandal, 2007; Cai, 2008 and Das, Mabrouk; Arthanareeswaran, 2020)

3.2 Cellular Automata Based Model of Nanorobots

As shown in the previous section, our model comprises two phases separated into distinct temporal stages in our CA algorithm. Once the tumour growth is achieved, the second stage of our experiment introducing a swarm of nanorobots is set. Many parameters need to be initialised since our simulation is based on a singular matrix of number with no extra layer to introduce the nanobots as floating particles. Hence, the need to add a new state or “number” representing the nanorobots shown in table 1. Moreover, the key assumptions and rules responsible for controlling the whole simulation are put in place in the following parts of this section, where additional work is also addressed.

3.2.1 Assumptions & Initialisation

Due to the type of simulation used in this paper, many assumptions need to be anticipated to ensure reliable and accurate control of the swarm. Considering that the movement of each bot is directed by a change in the matrix numbers, where each number incarnate a specific state and colour, the cells states at each iteration is crucial. Therefore, we assume that one cancerous cell starts its apoptosis if and only if one nanobot have trespassed the cell. When moving in the x -direction, the nanorobots are capable of healing both lower and adjacent upper cells at the next iteration. When progressing vertically, the particles are able to target the horizontally located cells. The grid's dimensions are fixed by boundaries conditions, halting further displacement of the nanoparticle along these lines. The nanorobots can only move to one of their four neighbours, i.e. either to the x or y -direction of the grid. Each nanorobot can only move to a single square per iteration/second. Finally, as we are using precise targeting treatment, we assume that when one cancerous cell is destroyed, another normal cell replaces it in the simulation. On the other hand, Before stating the control system of the nanoparticles, some parameters need to be pre-defined. The second time parameter delimitating the treatment phase is initiated. The user defines the number of nanorobots at the beginning of the simulation while their position is assigned vertically along the grid's first column. Lastly, both number and colour unique to the robots state are set.

0	0	0	0	0	0	0	0
0	0	0	0	0	3	0	0
0	0	1	0	0	0	0	0
0	1	1	1	1	0	0	0
0	0	1	1	0	0	0	0
0	3	0	1	0	0	0	0
0	0	0	0	0	0	3	0
0	0	0	0	0	0	0	0

Figure 9: A simplified version of the simulation displaying the different numbers and colours specific to each cell's state.

The remaining parameters are shown in table 2. A simplified version of the framework is illustrated in figure 9.

3.2.2 Rules: Nanorobots' Control Laws

The rules referred to in this section make up the nanorobots' control algorithm while considering the previously stated assumptions. Due to the particularity and singularity of each cancer, this study elaborates a unique tumour growth and location each time the

algorithm is run to train the bots to target any tumour. Hence, the complexity of the task since there are multiple possible scenarios and neighbours at each iteration. More than forty rules have been developed to deliver a panacea to tackle this problem and cover most of the possible scenarios and states encountered. Algorithm 2 shows some of the rules implemented, and a link to the repository where all the rules are stated is available in section 8.3.4.

The code implemented in this study supposes that if a nanorobot is surrounded by healthy cells, it will move to the left until coming across one of the tumoral cells. Once the tumour is located, the nanorobots work efficiently with the swarm to track most cancer cells. This ordered network arising from low-level interactions between members of an initially unstable system is similar to the self-organisation of mound-building termites (Werfel, Petersen and Nagpal, 2014). These termites colonies inspire energy-efficient construction characterised by local actions to produce collective high-level results using indirect communication methods.

Algorithm 2 Nanorobots kinetics rules

```

1: for  $t_i \in \{1, \dots, t_2\} \forall t > 0$  do
2:   for all  $cell \in Grid$  do
3:     if  $cell^t(x, y) = R \cap cell^t(x, y + 1) = C \cap cell^t(x + 1, y) = C \cap cell^t(x - 1, y) = C$ 
        then
4:        $cell^{t+1}(x, y) = D$ 
5:        $cell^{t+1}(x - 1, y) = D$ 
6:        $cell^{t+1}(x + 1, y) = D$ 
7:        $cell^{t+1}(x, y + 1) = R$ 
8:     end if
9:     if  $cell^t(x, y) = R \cap cell^t(x, y + 1) = N \cap cell^t(x + 1, y) = N \cap cell^t(x - 1, y) = N$ 
        then
10:       $cell^{t+1}(x, y + 1) = R$ 
11:    end if
12:    if  $cell^t(x, y) = R \cap cell^t(x, y + 1) = N \cap cell^t(x + 1, y) = C \cap cell^t(x - 1, y) = N$ 
         $\cap cell^t(x, y - 1) = C$  then
13:       $cell^{t+1}(x, y) = D$ 
14:       $cell^{t+1}(x, y - 1) = D$ 
15:       $cell^{t+1}(x, y + 1) = D$ 
16:       $cell^{t+1}(x + 1, y) = R$ 
17:    end if
18:    if  $cell^t(x, y) = R \cap cell^t(x, y + 1) = B \cap cell^t(x + 1, y) = C \cap cell^t(x - 1, y) = C$ 
         $\cap cell^t(x, y - 1) = N$  then
19:       $cell^{t+1}(x + 1, y) = D$ 
20:       $cell^{t+1}(x - 1, y) = R$ 
21:    end if
22:  end for
23: end for

```

3.2.3 Results & Future work

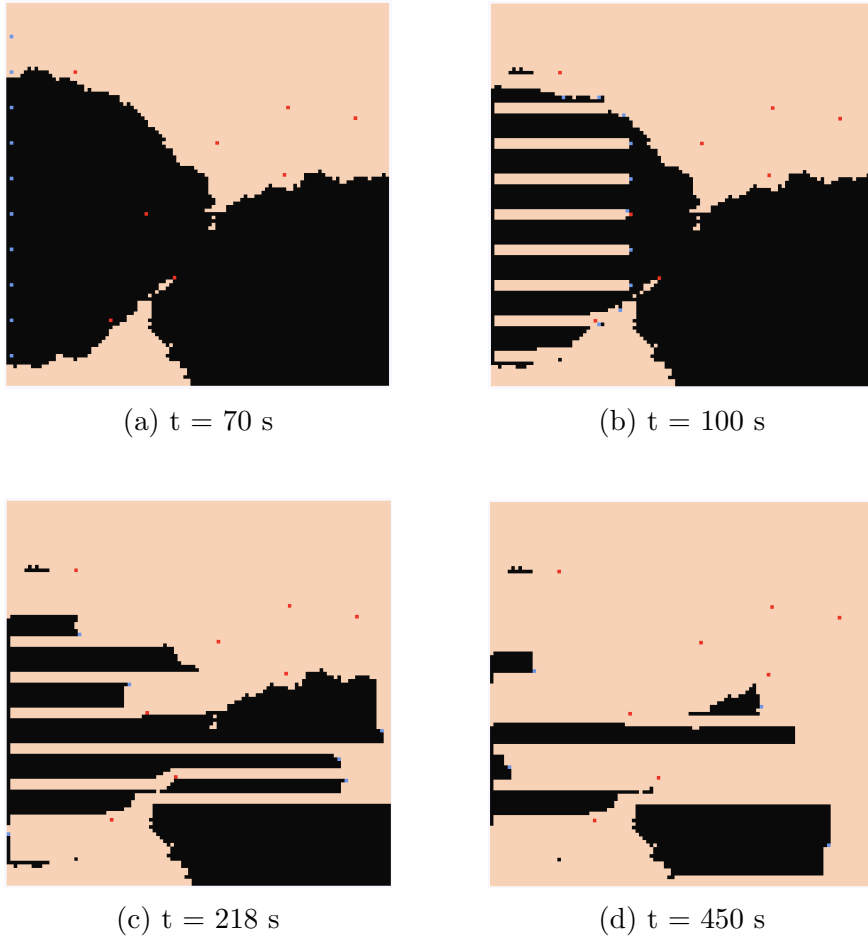


Figure 10: Single run of the treatment phase started from a complete tumour growth. The figures are ordered snapshots of the nanorobots movement in field at $t = 70\text{ s}$ (a), $t = 100\text{ s}$ (b), $t = 218\text{ s}$ (c), $t = 450\text{ s}$ (d).

Following many attempts and debugging procedures, the control algorithm was updated to cover most of the plausible scenarios. The overall progress of the model is available in the repository files of each simulation in section 8.4 (approximately 30 simulations were run). One of the final computational models can be observed in figure 10, where the nanorobots target the tumoral cells in the most efficient way possible. However, due to the complexity of the model and the type of system used, some errors keep occurring. Since all the robots possess the exact control mechanism dependent on their neighbours' type, and a range of motion limited to the horizontal or vertical direction in a 2D domain, they seem to converge to one entity in the grid. Meaning that the number of working agents is reduced every time two robots path overlaps. Other drawbacks appear to restrict the self-organisation of the robots, such as incomplete treatment of the tumour and stagnation of the particles since the algorithm does not cover the whole grid space.

Nevertheless, there exist some solutions to optimise the control system to make it more valid and reliable. One way to do that is by organising the algorithm to cover the whole grid area while ensuring that they do not cross the same trajectory. A new geometric algorithm can be generated to guide the agents directly towards the cancer cells via the minor path. For example, the A* search algorithm and Dijkstra algorithm are the most popular codes and theories for path-finding tasks and can be adapted to our simulation (Kapi, 2020). Another option would be to generate a unique control system for each nanobot, resolving the convergence issue. Finally, the best alternative would be to introduce the nanoparticles in a superposed layer under a multi-agent system instead of cell states. The following section will explore a multi-agent system alternative and generate four unique algorithms for cancer treatment using nanotechnology.

3.3 Multi-Agent based model of Nanorobots

Here comes the final programming phase of this research, where we will focus on designing a solid multi-agent-based model of nanorobots. The trajectory of the agents is iteratively updated to optimise cancer treatment while creating a highly ordered network within the environment. In order to achieve this function and avoid similar drawbacks to the previous algorithm, another software providing a specialised platform for multi-agent systems was required. The development environment in question is NetLogo, primarily written in Scala with some part in Java. The program allows different use of mobile agents known as turtles that circulate over a stationary cellular grid referred to as patches, equivalent to our cellular automata domain. This part focuses on developing a specialised control algorithm for our swarm of nanorobots inspired by swarm intelligence behaviour.

3.3.1 Assumptions & Initialisation

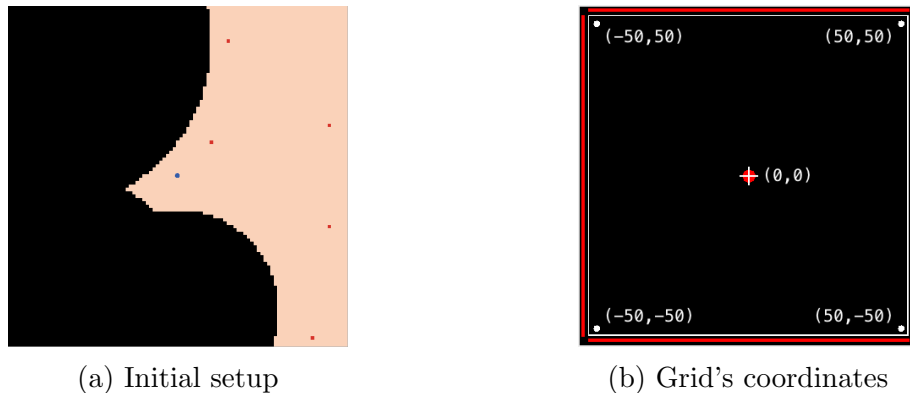


Figure 11: Grid's organisation including (a) outcome of the initial setup (b) size and coordinates of the domain.

Since the modelling environment was swapped to an adequate one to develop an efficient control algorithm for the nanorobots, a new set of parameters is initialised. Despite the possibility of integrating a cellular automata model in the new platform and having already programmed cancer growth beforehand, the main focus here is to test the efficacy of new control algorithms. The setup is the same for every code and involves modifying the patches to set a similar background domain to the first CA model. First, the agents/turtles are assigned a “dot” shape, a specific size comparable to the size of nanorobots and the colour blue. Then, the patches territory is defined by setting up the tumours areas as black circles along the grid depending on their radius and x y -coordinates of their centre. The grid size and organisation is shown in Figure 11b and the patches size set to 6.5 units. The rest of the patches were set as normal cells and blood bifurcations. Based on the cells type, corresponding colours were allocated to finalise the initialisation of our model, as shown in figure 11a. Considering the model’s limitations, assumptions equivalent to the one stated in section 3.2.1 are prescribed. The only difference here is that the agents are in an independent layer and can freely move around the framework. Once the initialisation is completed, the following steps consist of implementing our swarm’s control algorithm and comparing the outcome. In the next subsection, four algorithms are implemented.

3.3.2 Random Motion Algorithm

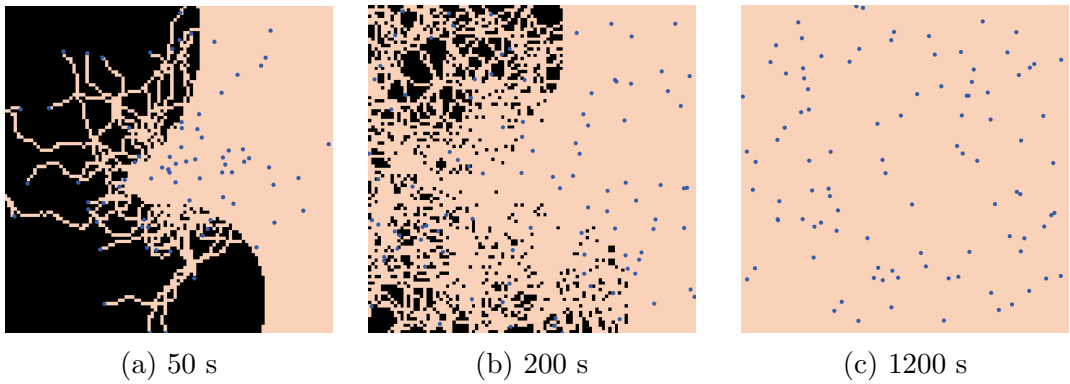


Figure 12: Random motion algorithm simulation showing different stage of the treatment at (a) $t = 50$ s, (b) $t = 200$ s and (c) $t = 1200$ s.

The random motion algorithm refers to the arbitrary movement of nanoparticles without involving any connection between the agents, i.e. each agent cannot sense the other members of the swarm and vary their direction accordingly. Nevertheless, the robots can differentiate between tumoral and normal cells and treat the malignant cells without sensing the cells prior to detecting them. This algorithm stands as control and landmark to compare the efficacy of the remaining problem-solving procedures. Figure 12 below shows the gradual progress of the swarm at three separate times until complete healing of

the tissue when assisted by the random motion algorithm. The only variable considered for this simulation is the swarm population.

3.3.3 Flock Motion Algorithm

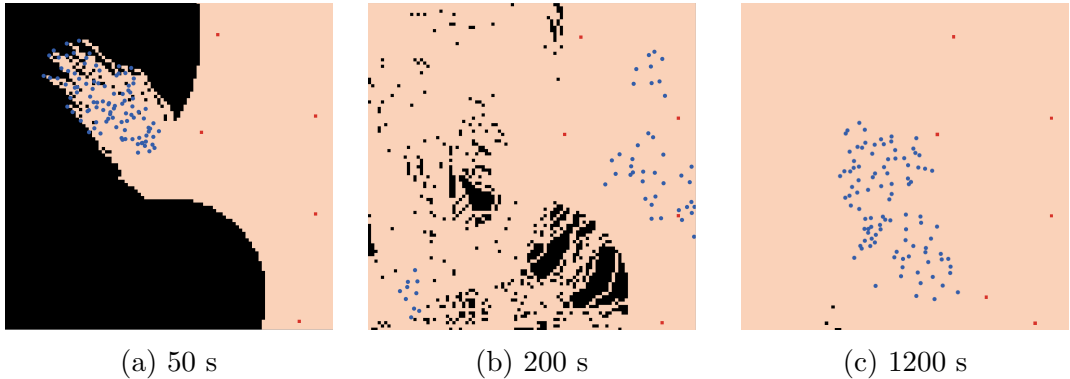


Figure 13: Flock motion algorithm simulation showing different stage of the treatment at (a) $t = 50$ s, (b) $t = 200$ s and (c) $t = 1200$ s.

The flock motion algorithm aims to copy the group migration of birds generally adopted for safety from predation and foraging benefits. Here, the nanorobots move in a flock shape by sensing the other swarm members present in their radius and alternating their direction suitably. The algorithm also allows the formation of more than one swarm, as seen in figure 13b where each agent can localise their nearest neighbour and the nearest swarm. Similarly to the previous algorithm, the nanorobots can differentiate between cancer and normal cells, but they cannot sense the cells prior to approaching them. Finally, the agents can either turn away or towards the closest nanorobot depending on their angle, where each small interaction strengthens the system's collective behaviour. Figure 13 below display the different stages involved in the simulation of the nanorobots respective to this algorithm. Three variables are considered, the swarm population, the nanobots radius of vision and the maximum alignment between robots.

3.3.4 Search Dominated Motion Algorithm

The search dominated algorithm is very similar to the flock motion of the nanoparticle in terms of programming; however, another piece of code is implemented to target the cancer cells. In addition to the ability of the nanorobots to sense their neighbours over a defined radius, the capabilities of the agents to detect cancerous cells was implemented. For the rest of the algorithms, the cancer detection area (or radius) was determined to allow the agents to sense all the cells available in the grid. Since the detection of both tumoral cells and neighbours is present in the remaining algorithms, the cancer targeting algorithm

investigates a more dominant research purpose, which means that each nanorobot first looks up for cancer cells before locating their nearest neighbour and forming a swarm. Figure 14 preview the evolution of the system at different steps, comparable to the CA system in python, and the same previous three variables are taken into account.

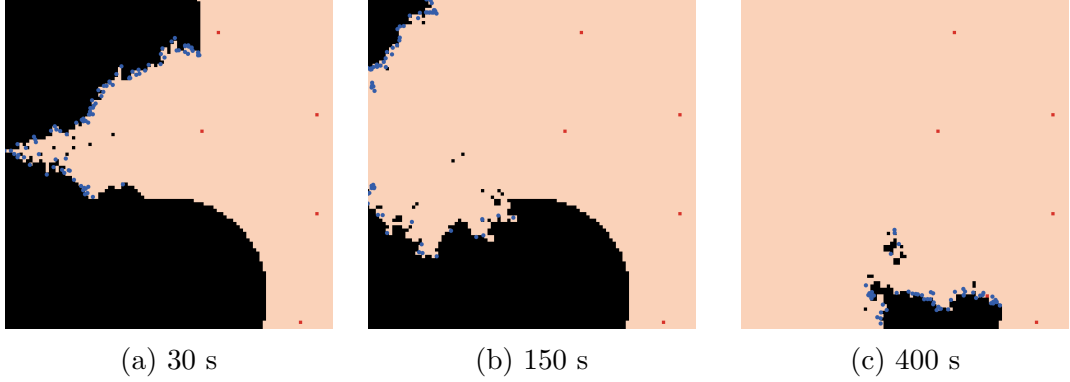


Figure 14: Search dominated algorithm simulation showing different stage of the treatment at (a) $t = 30$ s, (b) $t = 150$ s and (c) $t = 400$ s.

3.3.5 Flock Dominated Motion Algorithm

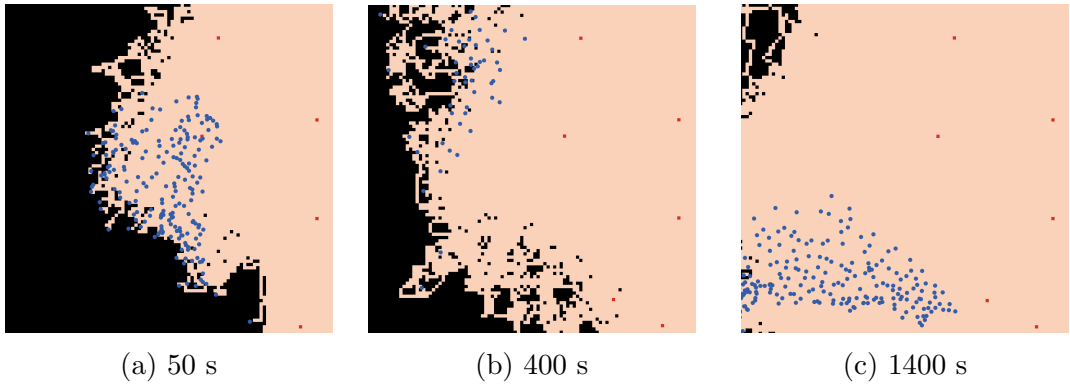


Figure 15: Flock dominated algorithm showing different stage of the treatment at (a) $t = 50$ s, (b) $t = 400$ s and (c) $t = 1400$ s.

This final algorithm is almost identical to the cancer targeting code, and the only contrast remains in the distribution of the nanoparticles tasks. In fact, instead of starting by targeting cancer cells, the flock dominated algorithm first sight to form a connected flock before searching for cancer cells. Figure 15 indicates the evolution of the swarm of nanorobots at different interval of time while considering the same three variables stated in section 3.3.3.

4 Results & Discussion

4.1 Variables Investigation

As discussed in section 3.3, three variables are investigated: the number of nanorobots, the agents' sensory radius and the alignment variable, controlling the separation and adjustment of the swarm. This section aims to determine the optimal value of each variable while investigating its effect on the different algorithms. In the next subsections, we will analyse the variables for a fixed swarm population and find the optimal control algorithm for this study.

4.1.1 50 Nanobots

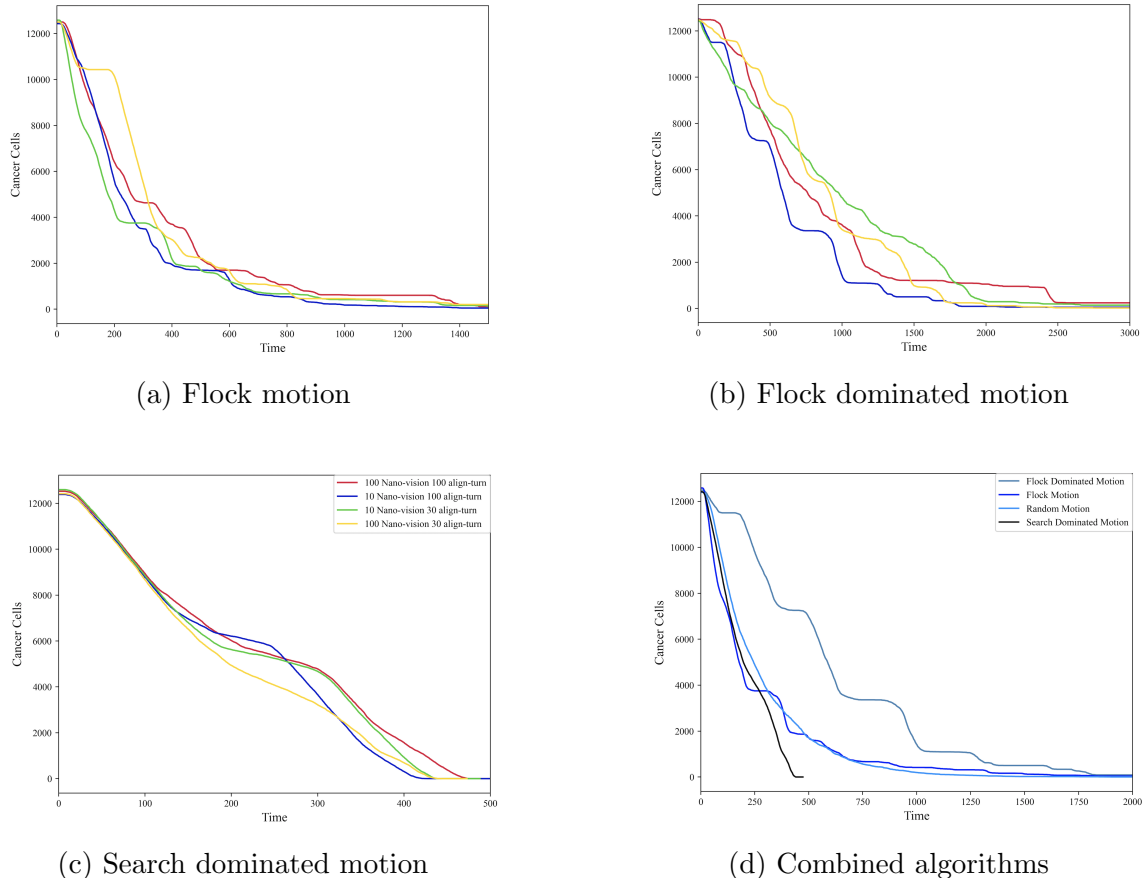


Figure 16: Variable analysis for 50 nanorobots for each algorithm (a) Flock motion, (b) Flock dominated motion, (c) Search dominated motion, (d) Combined algorithms. The red line (—) refers to 100 sensory radii and 100 align-turn, the blue line (—) refers to 10 sensory radii and 100 align-turn, the green line (—) refers to 10 sensory radii and 30 align-turn, and the yellow line (—) refers to 100 sensory radii and 30 align-turn.

Figure 16 shows the investigation of the variables for a swarm population of 50 nanorobots

where figure 16d combine the most efficient variable of each algorithm into one plot to allow further analysis. The flock motion simulation showed a similar trend for all variables in terms of time and efficacy for targeting the cancer cells while presenting some plateaux. These plateaux generally appear when the agents are not in contact with any cancer cells due to their inability to detect them. The dominated flock motion simulation favoured a low radius of detection and a high alignment value and presented large plateaux. The search dominated motion showed an almost identical efficiency for all variables with no plateaux since they are always actively targeting cancer cells. Finally, for 50 nanorobots, the combined outcomes revealed that the search dominated motion was the fastest and most efficient while the flock dominated motion revealed the most stagnation stages and slowest targeting. The flock and random motion showed matching curves and outcome.

4.1.2 100 Nanobots

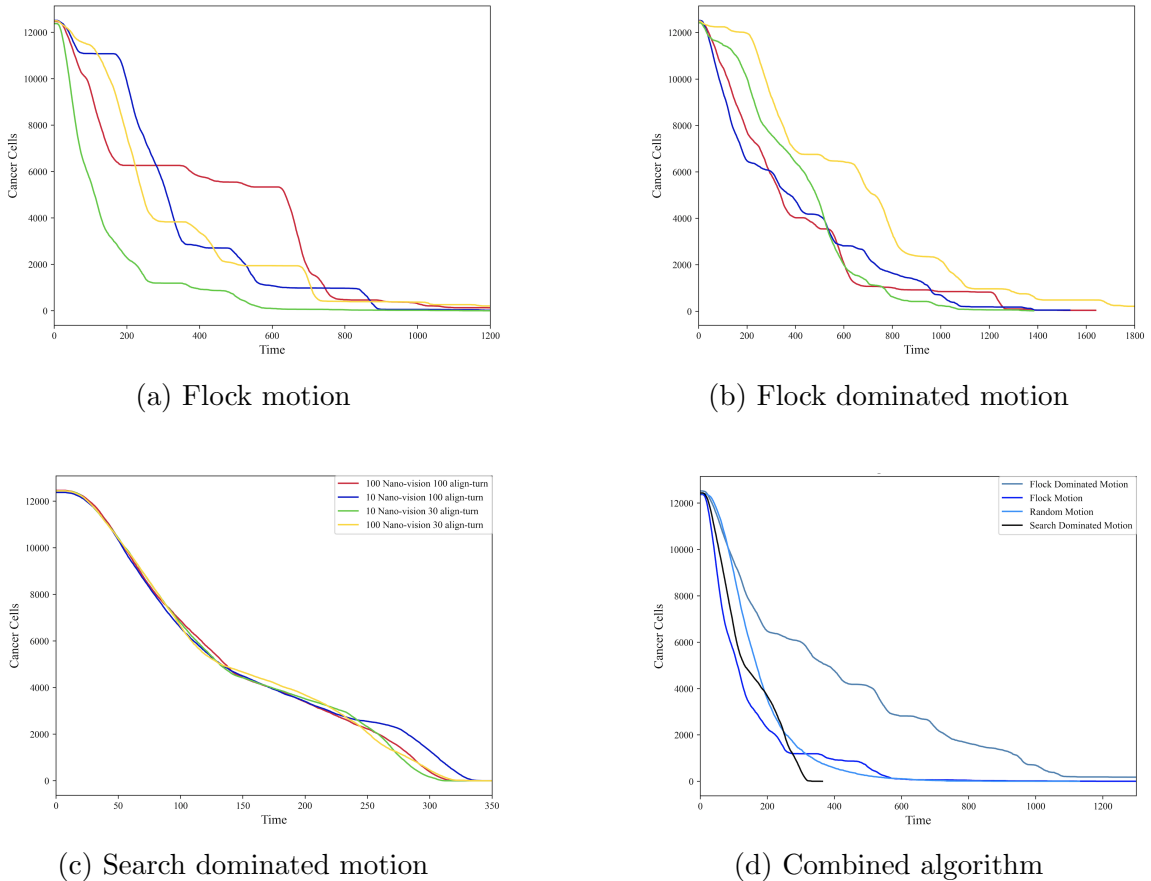


Figure 17: Variable analysis for 100 nanorobots for each algorithm (a) Flock motion, (b) Flock dominated motion, (c) Search dominated motion, (d) Combined algorithms. The red line (—) refers to 100 sensory radii and 100 align-turn, the blue line (—) refers to 10 sensory radii and 100 align-turn, the green line (—) refers to 10 sensory radii and 30 align-turn, and the yellow line (—) refers to 100 sensory radii and 30 align-turn.

Figure 17 investigate the change of variable for a population of 100 agents. Here, the flock motion simulation displays a specific cancer treatment with extensive stagnation phases and steep slopes. This trend reveals the swarm’s effectiveness to treat the disease when in contact with a tumour, yet their struggle at finding the targeted cells. For 100 nanorobots, a low nano-vision and alignment variable results with the best outcome. Figure 17b seems to obtain comparable curves, with the steeper curve at the lowest values of both variables and more plateau for high vision and small alignment variables. The search dominated motion disclose the same outcome as figure 16c while ensuring a faster treatment. The last plot 17d expose the most efficient outcome of each simulation, where the search dominant algorithm is the best overall in term of time and detection. On the other hand, the flock dominated algorithm showed less plateau with an increase in the population size.

4.1.3 150 Nanobots

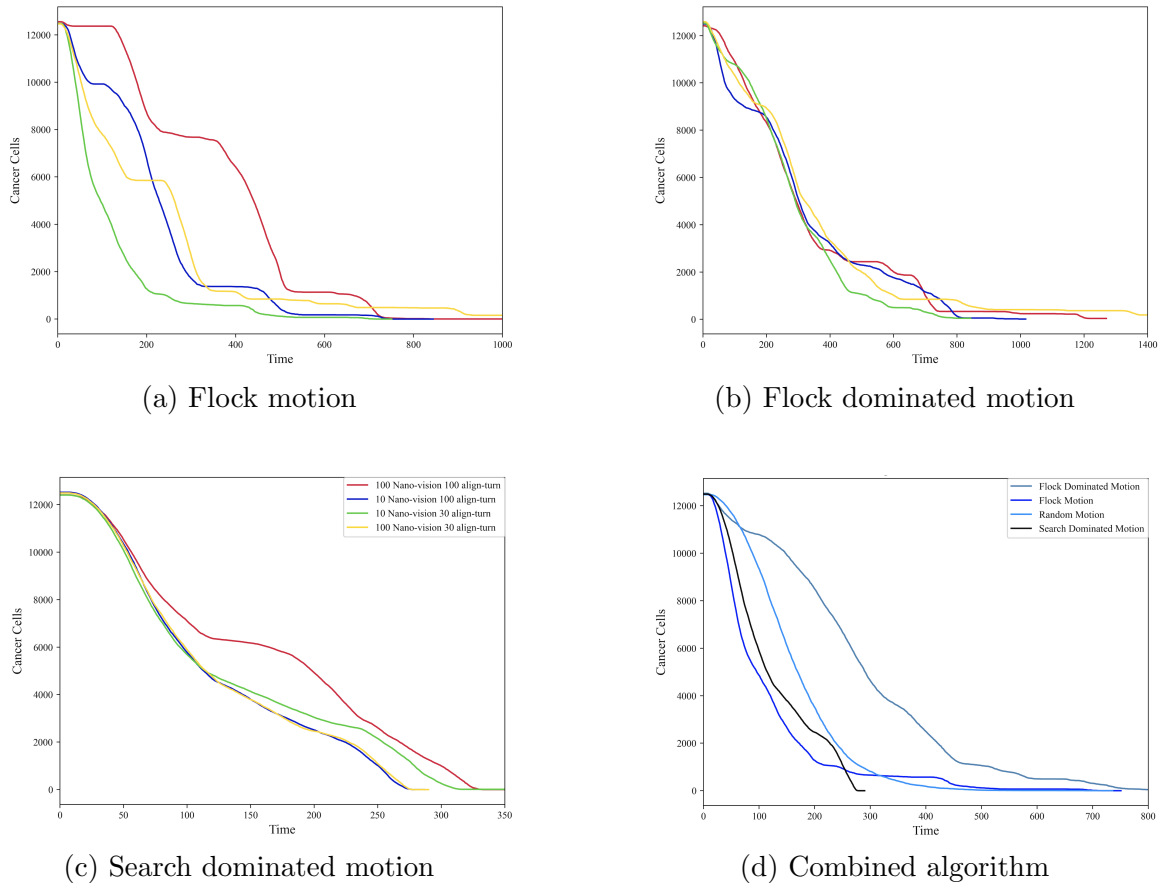


Figure 18: Variable analysis for 150 nanorobots for each algorithm (a) Flock motion, (b) Flock dominated motion, (c) Search dominated motion, (d) Combined algorithms. The red line (—) refers to 100 sensory radii and 100 align-turn, the blue line (—) refers to 10 sensory radii and 100 align-turn, the green line (—) refers to 10 sensory radii and 30 align-turn, and the yellow line (—) refers to 100 sensory radii and 30 align-turn.

For 150 nanorobots in figure 18, the flock motion algorithm shows a decrease in plateau and sharper slopes. The best outcome is obtained for the lowest variables values and the worst results for both high variables. The flock dominated motion is optimised with an increase in agents since the lines seem to present smaller plateaux and tighter trends. The simulation for the low variable's value is the most effective method to treat cancer cells. Nevertheless, the search dominated motion showed some disparities compared to the previous simulations. In effect, the red line referring to high variables values reveal a small plateau at 150 s caused by the travelling of the swarm from one end of the grid to the other where cancer cells are available. However, since we do not observe the same trend in figure 19c, we can conclude that the plateaux only appear when the swarm navigates through the grid and does not present a significant change. Finally, overall, the combined plot shows a smoother and steeper plot, and the flock motion presents a faster initial targeting before slowing down for a smaller number of cancer cells. The cancer research algorithm is still the most efficient for 150 agents due to the ability of the nanorobots to directly target and attack the cancerous cell before reorganising as a swarm.

4.1.4 200 Nanobots

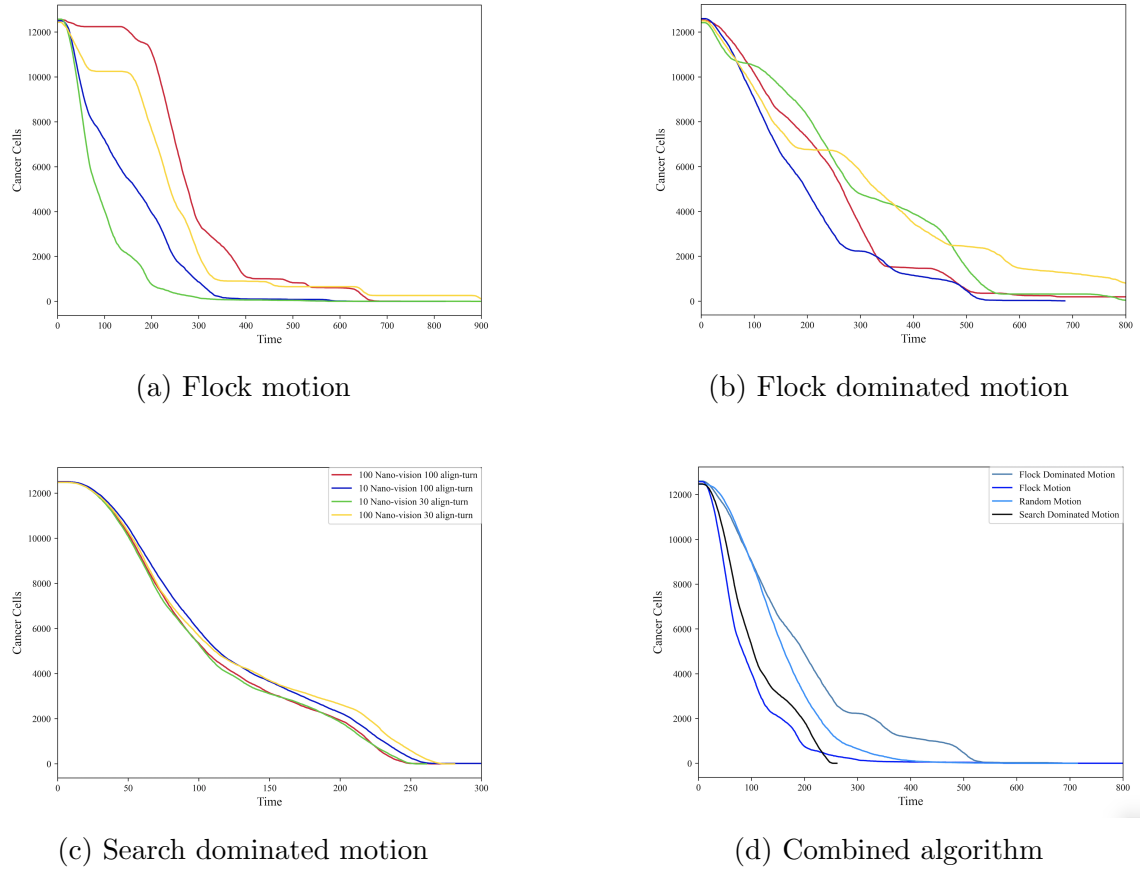


Figure 19: Variable analysis for 200 nanorobots for each algorithm (a) Flock motion, (b) Flock dominated motion, (c) Search dominated motion, (d) Combined algorithms. The red line (—) refers to 100 sensory radii and 100 align-turn, the blue line (—) refers to 10 sensory radii and 100 align-turn, the green line (—) refers to 10 sensory radii and 30 align-turn, and the yellow line (—) refers to 100 sensory radii and 30 align-turn.

To conclude the numerical experiments for this study, and after briefly analysing the outcome obtained for 200 agents, we close this section with an overall interpretation of the results. In fact, for the larger swarm size, a significant decrease in plateaux and steeper slopes are shown in figure 19 with smoothed down curves. The outcome of the flock motion algorithm exhibits matching patterns to previous plots, where the lowest variables still provide the best result. The flock dominated algorithm here reveal a better outcome for the blue line, low vision and high alignment, instead of the green line, low vision and low alignment. Figure 19c and 19d present similar general pattern from the previous one with lower population size.

Overall, we can observe some significant trends by alternating the values of the variables and increasing the number of nanorobots, respectively. We observed that by increasing the swarm population, the flock motion algorithm decreased in number and plateaux, induced steeper lines and faster treatment time. This observation can be explained by the larger area covered as the swarm grows in number and hence less time not active. The green line referring to the lowest radius of vision and alignment variable of the nanorobots stand out from the other, being the most effective combination for the flock motion.

In fact, a lower radius of detection allows the agents to focus on a limited number of agents to form a swarm, hence leading to a higher number of small flocks randomly circulating and covering the grid area. A lower alignment variable value (η) indicate a minor change in direction. Concerning the flock dominated motion, on top of the similar plateaux and time observations, we notice more resemblant curves as the number of nanorobots increase. The search dominated motion does not reveal significant changes by varying the different variables besides small fluctuations in ending time, from 500 s for 50 agents to 300 s for 200 agents. The reasoning behind these results is caused by the variables in question that mainly affect the swarm formation, whereas this algorithm prioritises the targeting of cancer cells rather than the flock formation. The simulations starting with a steep fall in the number of cancer cells and a long end time is due to the inability of the robots to sense the cancer cells before attacking them since their movement is mainly random aside from the search dominated algorithm.

In closing, the combined figure displays each simulations optimal outcome for the same number of nanobots. With an increase in the swarm size, it is seen that the trend of the curves highly resembles each other, with the only difference related to the start of rapid targeting of tumoral cells [figure 19]. The most influenced algorithm with the increase in population is the flock dominated motion, whereas the less modified one is the search dominated algorithm.

Section 8.1 provides the analysis of other real-life problems that can be solved through the swarm robotic algorithms implemented.

5 Conclusions

Cancer-related deaths keep rising in frequency and severity around the world, having a significant impact on society. The current types of cancer treatments are still evolving and embrace many side effects that deteriorate patients quality of life. Modern therapies have tested the effect of nanoparticles on the detection and diagnosis of tumoral cells but scarcely engaged swarm of nanorobots for targeting and drug delivery. This paper studied the potential of a new treatment through self-organising swarms of nanorobots and analyse the efficiency of control algorithms influenced by the cooperative behaviour of social animals. The main focus here was the modelling of a control algorithm that induces proper self-organisation of the swarm to obtain the desired cancer targeting behaviour and not the physical design of nanorobots. In the first part of this study, a cellular automata-based model of cancer growth coupled with a rule dominated algorithm for swarms of nanorobots was adapted on a 2D matrix environment. Despite the defects emerging from the CA model, a second simulation platform was used to test the outcome of four new control algorithms on cancer targeting. The experiments completed in section 4 compared the effects of different variables on the performance of every simulation and supplied some perception into potential variables to control the functioning of the swarm. In the last part of the paper, the ability of a swarm of robots to decontaminate a pollution source was evaluated using the search-based algorithm while investigating the speed and size factor on the application. It can be concluded that the collective behaviour of a multi-agent system of nanorobots is a robust and promising line of study to provide a novel therapy to treat metastatic cancer.

6 Contributions & Acknowledgements

I would like to extend my deepest gratitude to my supervisor Dr Ketao Zhang for his relentless support, unparalleled knowledge and profound belief in my work. I am extremely grateful for his guidance and support throughout the duration of this project, constantly providing me with insightful suggestions. I am also deeply indebted to Navin Patel for his unwavering support and extended assistance in creating valid mathematical equations to back up my algorithms.

Finally, I cannot conclude this study without mentioning my parents and family, without whom the completion of my work would not have been possible; I am forever grateful for nurturing me with encouragement and forbearance.

7 References

- A, S., D, D. and J, S., 2018. Nanorobots in Cancer Treatment. International Journal of Trend in Scientific Research and Development, Volume-2 (Issue-5), pp.117-120.
- Ahmad, H., n.d. Multi-agent systems: overview of a new paradigm for distributed systems. 7th IEEE International Symposium on High Assurance Systems Engineering, 2002. Proceedings.
- Anderson, A., Chaplain, M., Newman, E., Steele, R. and Thompson, A., 2000. Mathematical Modelling of Tumour Invasion and Metastasis. *Journal of Theoretical Medicine*, 2(2), pp.129-154.
- Anderson, D. R., Burnham, K. P., & Thompson, W. L. (2000). Anderson et al 2000.pdf. In *Journal of Wildlife Management*.
- Armstrong, T. S., Mendoza, T., Gring, I., Coco, C., Cohen, M. Z., Eriksen, L., Hsu, M. A., Gilbert, M. R., & Cleeland, C. (2006). Validation of the M.D. Anderson symptom inventory brain tumor module (MDASI-BT). *Journal of Neuro-Oncology*.
- Arruebo, M., Vilaboa, N., Sáez-Gutierrez, B., Lambea, J., Tres, A., Valladares, M. and González-Fernández, Á., 2011. Assessment of the Evolution of Cancer Treatment Therapies. *Cancers*, 3(3), pp.3279-3330.
- Bayda, S., Adeel, M., Tuccinardi, T., Cordani, M. and Rizzolio, F., 2019. The History of Nanoscience and Nanotechnology: From Chemical–Physical Applications to Nanomedicine. *Molecules*, 25(1), p.112.
- Bayda, S., Adeel, M., Tuccinardi, T., Cordani, M., & Rizzolio, F. (2020). The history of nanoscience and nanotechnology: From chemical-physical applications to nanomedicine. In *Molecules*.
- Brannon-Peppas, L., & Blanchette, J. O. (2012). Nanoparticle and targeted systems for cancer therapy. In *Advanced Drug Delivery Reviews*.
- Butler, J., Mackay, F., Denniston, C. and Daley, M., 2014. Simulating Cancer Growth Using Cellular Automata to Detect Combination Drug Targets. *Unconventional Computation and Natural Computation*, pp.67-79.
- Byrne, H. M. (2010). Dissecting cancer through mathematics: From the cell to the animal model. In *Nature Reviews Cancer*.
- Cai, W., 2008. Applications of gold nanoparticles in cancer nanotechnology. *Nanotechnology, Science and Applications*, Volume 1, pp.17-32.
- Cerruti, U., Dutto, S. and Murru, N., 2020. A symbiosis between cellular automata and genetic algorithms. *Chaos, Solitons & Fractals*, 134, p.109719.
- Chythanya C. Kutty, Amit B. Patil, Asha Spandana K M, Gowda D M and Preeti S, 2020. Nanorobots in Cancer Therapy. *International Journal of Research in Pharmaceutical Sciences*, 11(3), pp.3626-3636.

- Das, D., Mabrouk, M., Beherei, H. and Arthanareeswaran, G., 2020. Pharmaceutical Particulates and Membranes for the Delivery of Drugs and Bioactive Molecules. *Pharmaceutics*, 12(5), p.412.
- De Jong, W. H., & Borm, P. J. A. (2008). Drug delivery and nanoparticles: Applications and hazards. In *International Journal of Nanomedicine*.
- Dolev, S., Narayanan, R. and Rosenblit, M., 2019. Design of nanorobots for exposing cancer cells. *Nanotechnology*, 30(31), p.315501.
- Duan, J., Zhu, Y. and Huang, S., 2012. Stigmergy agent and swarm-intelligence-based multi-agent system. Proceedings of the 10th World Congress on Intelligent Control and Automation.,
- Düchting, W. and Dehl, G., 1980. Spread of cancer cells in tissues: Modelling and simulation. *International Journal of Bio-Medical Computing*, 11(3), pp.175-195.
- El Naqa, I., & Murphy, M. J. (2015). What Is Machine Learning? In *Machine Learning in Radiation Oncology*.
- Ferlay, J., Soerjomataram, I., Ervik, M., Dikshit, R., Eser, S., Mathers, C., Rebelo, M., Parkin, D., Forman, D., & Bray, F. (2013). GLOBOCAN 2012 v1.0, Cancer Incidence and Mortality Worldwide. Lyon, France: International Agency for Research on Cancer.
- Franssen, L. C., Lorenzi, T., Burgess, A. E. F., & Chaplain, M. A. J. (2019). A Mathematical Framework for Modelling the Metastatic Spread of Cancer. *Bulletin of Mathematical Biology*.
- Gardner, M., 1966. Mathematical Games. *Scientific American*, 215(3), pp.264-272.
- Gardner, Martin (October 1970). "Mathematical Games - The Fantastic Combinations of John Conway's New Solitaire Game 'Life'" (PDF). *Scientific American* (223): 120–123
- Gerisch, A. and Chaplain, M., 2008. Mathematical modelling of cancer cell invasion of tissue: Local and non-local models and the effect of adhesion. *Journal of Theoretical Biology*, 250(4), pp.684-704.
- Hadeler, K. and Müller, J., 2017 Cellular Automata: Analysis and Applications.
- Hanahan D, Weinberg RA. The hallmarks of cancer. *Cell*. 2000;100(1):57-70.
- Innocente, M. and Grasso, P., 2019. Self-organising swarms of firefighting drones: Harnessing the power of collective intelligence in decentralised multi-robot systems. *Journal of Computational Science*, 34, pp.80-101.
- jabbar, M., Deekshatulu, B. and Chandra, P., 2013. Classification of Heart Disease Using K- Nearest Neighbor and Genetic Algorithm. *Procedia Technology*, 10, pp.85-94.

Jeremy Jordan (2017). Convolutional neural networks. In Jeremy Jordan. Accessed 8 November 2020. <https://www.jeremyjordan.me/convolutional-neural-networks/>

Kansal, A. R., Torquato, S., Harsh IV, G. R., Chiocca, E. A., & Deisboeck, T. S. (2000). Simulated brain tumor growth dynamics using a three-dimensional cellular automaton. *Journal of Theoretical Biology*.

Kapi, A., 2020. A Review on Informed Search Algorithms for Video Games Pathfinding. *International Journal of Advanced Trends in Computer Science and Engineering*, 9(3), pp.2756-2764.

Madou, M., 2012. Manufacturing techniques for microfabrication and nanotechnology. Boca Raton [etc.]: CRC Press.

Margarit, D. H., & Romanelli, L. (2016). A mathematical model of absorbing Markov chains to understand the routes of metastasis. *BIOMATH*.

Mc Carthy, D. J., Malhotra, M., O'Mahony, A. M., Cryan, J. F., & O'Driscoll, C. M. (2015). Nanoparticles and the blood-brain barrier: Advancing from in-vitro models towards therapeutic significance. *Pharmaceutical Research*.

Medium. 2019. How to simulate Wildfires with Python. [online] Available at: <https://medium.com/@PedroLFerreira/how-to-simulate-wildfires-with-python-6562e2eed266> [Accessed September 2020].

Miller, J. and Ting, T., 2019. EoN (Epidemics on Networks): a fast, flexible Python package for simulation, analytic approximation, and analysis of epidemics on networks. *Journal of Open Source Software*, 4(44), p.1731.

Murphy, H., Jaafari, H. and Dobrovolny, H., 2016. Differences in predictions of ODE models of tumor growth: a cautionary example. *BMC Cancer*, 16(1).

Muzy, A., Innocenti, E., Aiello, A., Santucci, J. and Wainer, G., 2005. Specification of Discrete Event Models for Fire Spreading. *SIMULATION*, 81(2), pp.103-117.

Natasha K. Martin, Eamonn A. Gaffney, Robert A. Gatenby, Philip K. Maini. Tumour-stromal inter- actions in acid-mediated invasion: A mathematical model. *Journal of Theoretical Biology*, Elsevier, 2010, 267 (3), pp.461.

National Cancer Institute (2017). Benefits of Nanotechnology for Cancer. In Cancer & Nanotech in Nanodelivery System and Devices Branch in National Cancer Institute. Accessed: 9 November 2020. <https://www.cancer.gov/nano/cancer-nanotechnology/benefits>

Navarro, I. and Matía, F., 2013. An Introduction to Swarm Robotics. *ISRN Robotics*, 2013, pp.1-10.

Newton, P. K., Mason, J., Bethel, K., Bazhenova, L., Nieva, J., Norton, L., & Kuhn, P. (2013). Spreaders and sponges define metastasis in lung cancer: A markov chain monte carlo mathematical model. *Cancer Research*.

O'Rourke, J., & Toussaint, G. T. (2017). Pattern recognition. In *Handbook of Discrete and Computational Geometry*, Third Edition.

Pearce, A., Haas, M., Viney, R., Pearson, S., Haywood, P., Brown, C. and Ward, R., 2017. Incidence and severity of self-reported chemotherapy side effects in routine care: A prospective cohort study. *PLOS ONE*, 12(10), p.e0184360.

Praetorius, N. and Mandal, T., 2007. Engineered Nanoparticles in Cancer Therapy. *Recent Patents on Drug Delivery & Formulation*, 1(1), pp.37-51.

Pucci, C., Martinelli, C. and Ciofani, G., 2019. Innovative approaches for cancer treatment: current perspectives and new challenges. *ecancermedicalscience*, 13.

Ramis-Conde, I., Chaplain, M. and Anderson, A., 2008. Mathematical modelling of cancer cell invasion of tissue. *Mathematical and Computer Modelling*, 47(5-6), pp.533-545.

Reséndiz-Benhumea, G., Froese, T., Ramos-Fernández, G. and Smith-Aguilar, S., 2019. Applying Social Network Analysis to Agent-Based Models: A Case Study of Task Allocation in Swarm Robotics Inspired by Ant Foraging Behavior. *The 2019 Conference on Artificial Life*.

Rubaek, T., Cikotic, M. And Falden, S., 2016. Evaluation of the UV-Disinfection Robot.

Sadeghi Amjadi, A., Raoufi, M., Turgut, A., Broughton, G., Krajník, T. and Arvin, F., 2021. Cooperative Pollution Source Exploration and Cleanup with a Bio-inspired Swarm Robot Aggregation. *Lecture Notes of the Institute for Computer Sciences, Social Informatics and Telecommunications Engineering*, pp.469-481.

Schroeder, A., Heller, D., Winslow, M., Dahlman, J., Pratt, G., Langer, R., Jacks, T. and Anderson, D., 2011. Treating metastatic cancer with nanotechnology. *Nature Reviews Cancer*, 12(1), pp.39-50.

Senanayake, M., Senthooran, I., Barca, J., Chung, H., Kamruzzaman, J. and Murshed, M., 2016. Search and tracking algorithms for swarms of robots: A survey. *Robotics and Autonomous Systems*, 75, pp.422-434.

Shiflet, Angela and George Shiflet. 2006. *Introduction to Computational Science: Modeling and Simulation for the Sciences*. Princeton: Princeton University Press: 576 pp.

ShuaiYuan (2014). How to use the actual feature names instead of "X" in scikit-learn DecisionTreeRegressor? Stack Overflow. Accessed 8 November 2020. <https://stackoverflow.com/questions/21420225/how-to-use-the-actual-feature-names-instead-of-x-in-scikit-learn-decisiontree>

Stewart BW, Wild CP, editors. *World cancer report 2014*. Lyon: International Agency for Research on Cancer; 2014.

Tan, Y. and Zheng, Z., 2013. Research Advance in Swarm Robotics. Defence Technology, 9(1), pp.18-39.

Tinoco, C., Lima, D. and Oliveira, G., 2017. An improved model for swarm robotics in surveillance based on cellular automata and repulsive pheromone with discrete diffusion. International Journal of Parallel, Emergent and Distributed Systems, 34(1), pp.53-77.

Trianni, V., IJsselmuiden, J., & Haken, R. (2016). The SAGA concept: Swarm Robotics for Agricultural Applications.

Van Dijkhuizen-Radersma, R., Moroni, L., Apeldoorn, A. van, Zhang, Z., & Grijpma, D. (2008). Degradable Polymers for Tissue Engineering. In Tissue Engineering.

Wang, J. (2018). Modeling Cancer Growth with Differential Equations.

Werfel, J., Petersen, K. and Nagpal, R., 2014. Designing Collective Behavior in a Termite-Inspired Robot Construction Team. Science, 343(6172), pp.754-758.

Wood, M. and DeLoach, S., 2001. An Overview of the Multiagent Systems Engineering Methodology. Agent-Oriented Software Engineering, pp.207-221.

Zhang, L., Gu, F., Chan, J., Wang, A., Langer, R. and Farokhzad, O., 2007. Nanoparticles in Medicine: Therapeutic Applications and Developments. Clinical Pharmacology & Therapeutics, 83(5), pp.761-769.

8 Appendix

8.1 Appendix A: Supplementary Work

Both the mathematical theory behind the control of the nanorobots and further applications tested are available at the link below:

<https://collect.qmul.ac.uk/down?t=4TS1J6QKBFDB0ODUKG/6H7IVCTGC7EB6USKHBN0280>

8.2 Appendix B: Parameters of the simulations

8.2.1 Cellular Automata Parameters

Table 2: Parameters of the cellular automata cancer model

Parameter	Description	Value/Range
N	normal cell	0
C	cancerous cell	1
B	grid's boundary cell	100
R	nanorobots particle	3
r	random generated number	[0,1]
t	simulation time	[100,900]
t_1	cancer growth simulation time	[0,100]
t_2	cancer growth simulation time	[100,900]
α	probability that the cancer grows south	0.5
β	probability that the cancer grows north	0.3
γ	probability that the cancer grows east	0.7
δ	probability that the cancer grows west	0.6

8.2.2 Multi-Agent system Parameters

Table 3: Parameters of the decontamination floor simulation.

Parameter	Description	Value/Range
r_v	radius of vision of robots	1000
η	alignment variable	[0,100]
D_{min}	minimum distance between robots	3
ν_r	robot's linear velocity	[0,1]
T	number of robots in the simulation	[0,50]

8.3 Appendix C: Algorithms Repository

8.3.1 Cancer Growth Algorithm

<https://collect.qmul.ac.uk/down?t=514DJIB6D7ABKVS0H0/4L0DRTRS7KSDV7FSC2T5ETO>

8.3.2 Accuracy of Cancer Growth Model

<https://collect.qmul.ac.uk/down?t=5542RCID88PTJ67HES/6P025CTGC7EB60C0JJSPGF8>

8.3.3 Cancer Population Plot

<https://collect.qmul.ac.uk/down?t=6T52LEBMF7I8KJT8N0/4HPGR0VOI66664BGTG4UFJ8>

8.3.4 Nanorobot CA Algorithm coupled with cancer growth

<https://collect.qmul.ac.uk/down?t=610DRTG9107UB57DFC/4T7ITDTSFNS9UNDSK32A028>

8.3.5 Random Motion Algorithm

<https://collect.qmul.ac.uk/down?t=6P5TNGRSEFH8GID6NG/6LE3H9CE8CPDJ6VUCA36MIO>

8.3.6 Flock Motion Algorithm

<https://collect.qmul.ac.uk/down?t=6TE3BBQ06SJCP3FAF0/55TGJ64RBRFRCPK5J7V9CC0>

8.3.7 Search Dominated Motion Algorithm

<https://collect.qmul.ac.uk/down?t=59U1J257L2ANMFIRP4/59THF7S46KGFF9E4B2VL4T0>

8.3.8 Flock Dominated Motion Algorithm

<https://collect.qmul.ac.uk/down?t=51V64JF2QL0DD6VKE8/R8UT3JQK0L00FDEK92NLQHG>

8.3.9 Decontamination Floor Algorithm

<https://collect.qmul.ac.uk/down?t=6L42FD2B9J4QUOLVKK/4501744J80RTT7NTC60H3C0>

8.3.10 Variable Analysis Algorithm

<https://collect.qmul.ac.uk/down?t=45VHT0LTMAHKI2310S/6P735ELPF3I00I5BMVF0UDG>

8.4 Appendix D: CA Simulations

Simulation 1 Link

Simulation 2 Link

Simulation 3 Link

Simulation 4 Link

Simulation 5 Link

Simulation 6 Link

Simulation 7 Link

Simulation 8 Link

Simulation 9 Link

Simulation 10 Link

Simulation 11 Link

Simulation 12 Link

Simulation 13 Link

Simulation 14 Link

Simulation 15 Link

Simulation 16 Link

Simulation 17 Link

Simulation 18 Link

Simulation 19 Link

Simulation 20 Link

8.5 Appendix E: Cancer growth Data

Table 4: Cancer growth data of a Chinese hamster V79 fibroblast tumor.

t (days)	V ($10^9 \mu m^3$)	t	V	t	V	t	V	t	V
3.46	0.0158	12.39	0.4977	24.33	3.2046	35.2	5.9668	49.24	7.4971
4.58	0.0264	13.42	0.6033	25.58	4.5241	36.34	6.6945	50.19	7.5
5.67	0.0326	15.19	0.8441	26.43	4.3459	37.29	6.6395	51.14	7.402
6.64	0.0445	16.24	1.2163	27.44	5.1374	38.5	6.8971	52.1	7.25
7.63	0.0646	17.23	1.447	28.43	5.5376	39.67	7.2966	54	7.442
8.41	0.0933	18.18	2.3298	30.49	4.8946	41.37	7.2268	56.33	7.32
9.32	0.1454	19.29	2.5342	31.34	5.066	42.58	6.8815	57.33	7.356
10.27	0.2183	21.23	3.0064	32.34	6.1494	46.38	7.2112	59.38	7.4
11.19	0.2842	21.99	3.4044	33	6.8548	48.29	7.0694		